Thermal Conductance of Thin Silicon Nanowires

Renkun Chen,[1] Allon I. Hochbaum,[2] Padraig Murphy,[3] Joel Moore,[3,5] Peidong Yang,[2,4,5] and Arun Majumdar[1,4,5,*]

[1]*Department of Mechanical Engineering, University of California, Berkeley, California 94720, USA*
[2]*Department of Chemistry, University of California, Berkeley, California 94720, USA*
[3]*Department of Physics, University of California, Berkeley, California 94720, USA*
[4]*Department of Materials Science and Engineering, University of California, Berkeley, California 94720, USA*
[5]*Materials Sciences Division, Lawrence Berkeley National Laboratory, Berkeley, California 94720, USA*

(Received 11 February 2008; published 2 September 2008)

The thermal conductance of individual single crystalline silicon nanowires with diameters less than 30 nm has been measured from 20 to 100 K. The observed thermal conductance shows unusual linear temperature dependence at low temperatures, as opposed to the T^3 dependence predicted by the conventional phonon transport model. In contrast to previous models, the present study suggests that phonon-boundary scattering is highly frequency dependent, and ranges from nearly ballistic to completely diffusive, which can explain the unexpected linear temperature dependence.

DOI: 10.1103/PhysRevLett.101.105501 PACS numbers: 63.22.Gh, 65.80.+n, 66.70.Lm

One-dimensional semiconductor nanowires (NWs) have drawn significant attention in the past decade. These wires exhibit a strong size dependence of their electronic and optical properties [1,2], which leads to potential applications in nanoelectronics, photonics, and energy conversion [3–6]. In particular, there has been a growing interest in thermal properties of one-dimensional (1D) nanostructures including carbon nanotubes (NTs) [7] and NWs [8–17]. A detailed understanding of the thermal transport is crucial for potential applications such as thermoelectric power generation or cooling [5] and thermal management of electronics [18].

Although there have been a few reports on the thermal conductivity (k) measurement of individual semiconductor nanowires [8–12], nanowires investigated in these studies were relatively thick, such that they are still much larger than the dominant phonon wavelength $\lambda_{\max}$ [19]. As a result, the mean free path due to phonon-boundary scattering can normally be assumed to be the same for all the phonon modes. Theories based on the assumption that the mean free path is proportional to the nanowire diameter and independent of the phonon frequency were able to explain the observed experimental results of NWs with large diameters [13–16]. However, to the best of our knowledge, there has been no systematic experimental study on thermal transport properties of thin SiNWs with diameters comparable to $\lambda_{\max}$ at low temperature. The only available data on the 22 nm SiNW by Li *et al.* [8] yielded k significantly lower than the theoretical prediction and showed unusual linear temperature dependence from 20 K to room temperature, as opposed to the T^3 dependence expected from the well-known Debye model at low temperature. Attempts were made [20,21] to explain the unusual linear behavior of $k(T)$ as well as the unusually low k observed in Ref. [8], but the modeling results did not quantitatively agree with the experimental data. It is, therefore, important to systematically examine the phonon transport in thin SiNWs both experimentally and theoretically, in order to understand the underlying physics. Here we report a systematic study on thermal conductance $G(T)$ of thin SiNWs, which showed unusual linear temperature dependence. A theoretical model was developed to explain the observed $G(T)$ and suggests that phonon-boundary scattering is frequency dependent.

Thin SiNWs characterized in this study were synthesized by two methods, both based on metal-catalyzed chemical vapor deposition (CVD) growth [22]. In the first method, thin SiNWs were obtained by a diameter reduction approach, which is shown schematically in Fig. 1(a). SiNWs were first synthesized by vapor-liquid-solid (VLS) growth on Si substrates in a quartz-tube furnace, as described previously [23]. Using 50 nm Au nanoparticles as catalysts yielded arrays of epitaxially grown, single crystalline SiNWs with controlled diameters of roughly 90 nm [Fig. 1(b)]. Nanowire arrays were briefly dipped in 10:1 buffered hydrofluoric acid (BHF) and then an aqueous iodine and potassium iodide solution for at least 20 min to dissolve the Au catalyst particles. The array substrates were then rinsed in water and cleaned in an O_2 plasma at 300 W for 2 min. The NWs were oxidized at 850 °C in O_2 at atmospheric pressure for several hours to yield single crystalline SiNW cores of roughly 20 nm in diameter surrounded by a silica shell [Fig. 1(c)]. The single crystalline NW cores were released from the oxide shells by vapor HF etching above a bath of 50% HF [Fig. 1(d)]. Silicon nanowires synthesized by this method tend to be tapered, as the diameter gradually increases from below 20 nm at the tip to 30–40 nm at the base. In the second method, SiNWs below 20 nm in diameter were synthesized directly from 9 nm Pt nanoparticle catalysts by a similar CVD growth method [24]. The as-grown Pt-catalyzed

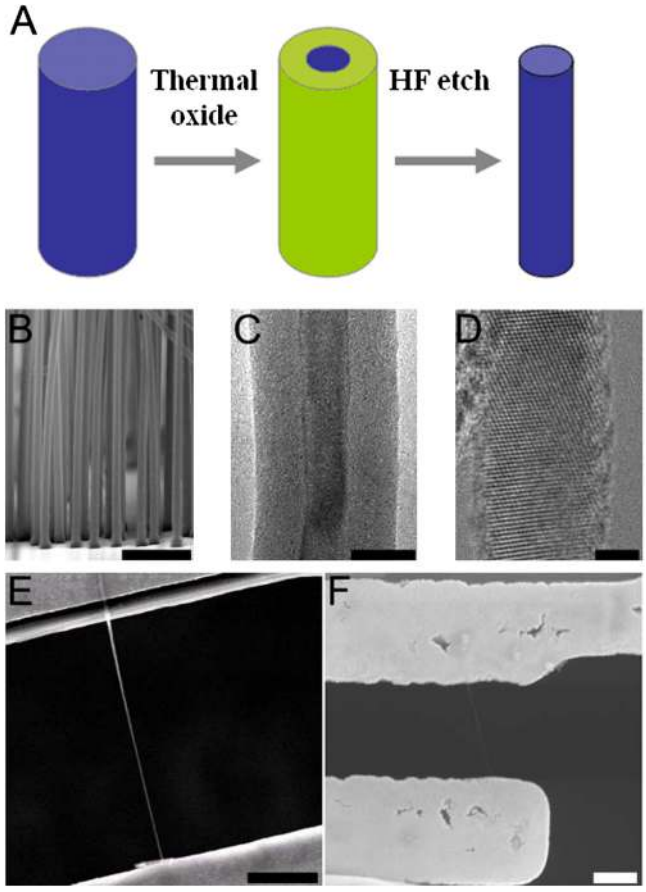

FIG. 1 (color online). (a) Schematic diagram of the diameter reduction method for making thin SiNWs: (b)–(d) electron microscope micrographs of SiNWs after VLS synthesis (b), thermal oxidation, (c) and oxide removal (d); scale bars are 1 μm, 30 nm, and 3 nm, respectively. (e) A bridging diameter-reduced SiNW; scale bar is 1 μm. (f) A bridging as-grown Pt-catalyzed SiNW; scale bar is 1 μm.

SiNWs were relatively uniform with diameters of 17.9 $\pm$ 3.1 nm, as determined by TEM analysis [24].

In order to study the diameter dependence of the thermal conductance, four diameter-reduced samples (#1 to #4) and two as-grown Pt-catalyzed samples (#5 and #6) of thin SiNWs were characterized in the present study (Table I). The length and diameter of each NW sample were determined by scanning electron microscopy (SEM) after the wires were placed on the measurement devices. For the diameter-reduced SiNWs, the diameter range given in Table I represents the diameters from the tip to the base of each tapered wire. For the as-grown Pt-catalyzed SiNWs, the range of diameters was approximately 15–20 nm. Because the resolution limit of the SEM could lead to significant error in k determination, only the thermal conductance is reported, and the diameters are meant mainly as guides for indexing different wire samples.

TABLE I. A summary of SiNW samples used in the present study.

	Diameter-Reduced				As-grown	
Sample #	1	2	3	4	5	6
$L(\mu m)$	2.21	2.51	2.68	4.54	1.71	2.24
D (nm)	31–50	26–34	20–29	24–30	15–20	15–20

We followed the measurement procedure summarized in Refs. [8,25]. Briefly, the thermal conductance (G) of individual NWs was characterized by micro-fabricated devices consisting of two suspended silicon nitride pads with integrated Pt line resistors serving as both heaters and resistive thermometers. After the thin NWs were dispersed onto the microdevices, SEM was used to find devices with individual thin NWs bridging the two pads [see Figs. 1(e) and 1(f)]. In order to improve the thermal contact between the wires and the suspended pads, nanowires were further bonded to the two pads by deposition of either an amorphous carbon film within a SEM or a Pt-C composite with the electron beam of a FEI Strata 235 Dual Beam FIB system. The thermal conductance of NWs was then measured from 20 K to room temperature (up to 400 K for sample 1). Figure 2(a) shows $G(T)$ for diameter-reduced SiNWs (#1 to #4) and as-grown Pt-catalyzed SiNWs (#5 and #6). For all the thin SiNW samples studied here, the thermal conductance $G(T)$ is generally lower for thinner wires, indicating strong phonon-boundary scattering throughout the temperature range, which was also observed previously in thick semiconductor nanowires [8–11]. However, the observed $G(T)$ initially increases with increasing temperature from 20 K to around 200 K, and then becomes flat or decreases at higher temperature for samples #1 and #2, indicating the onset of *umklapp* scattering, which was absent for the 22 nm SiNW in Ref. [8], where $k(T)$ increased linearly up to room temperature.

More interestingly, as shown in Fig. 2(b) in a log-log scale at low temperature (20 to 100 K), the observed $G(T)$ scales approximately linearly with temperature for all thin SiNW samples. This observation is consistent with what has been reported for the 22 nm SiNW in Ref. [8], but within a smaller temperature range. The observed linear $G(T)$ is not a result of ballistic and quantized phonon transport in 1D channels [26], since the temperature range studied here ($\geq$20 K) is much higher than the 1D crossover temperature for a 20 nm SiNW, which is around 8 K according to Ref. [26]. For bulk silicon, conventional phonon scattering theory predicts a T^3 dependence for low T thermal conductance, where the phonon mean free path is assumed to be a constant in the boundary scattering dominant regime [27].

To understand the observed phonon transport behavior in thin SiNW, we have developed a theoretical model that is based on the Landauer expression of the thermal conductance of a cylinder with boundary scattering in terms of the transmission probabilities of different modes of the cylinder. At the lowest frequencies, these phonons become

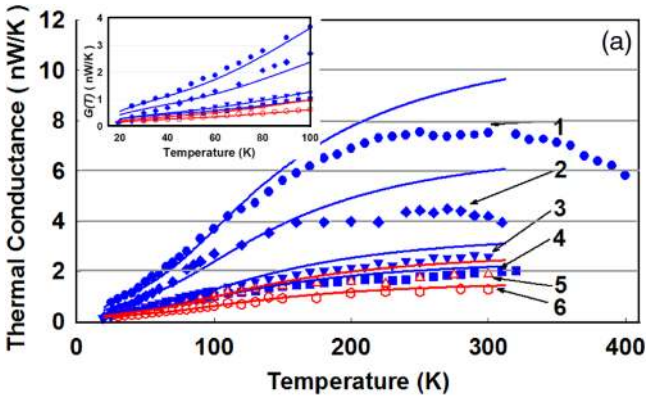

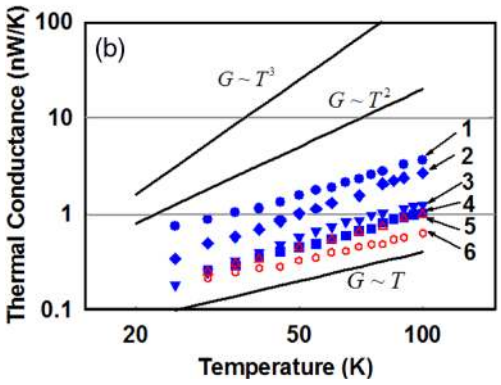

FIG. 2 (color online). (a) Thermal conductance $G(T)$ of thin VLS SiNWs. The number beside each curve denotes the sample number shown in Table I. Solid and open symbols represent the $G(T)$ for diameter-reduced and Pt-catalyzed as-grown SiNWs, respectively. The solid lines are the corresponding modeling results. Inset: Measured and calculated $G(T)$ from 20 to 100 K. (b) The $G(T)$ in log-log scale from 20 to 100 K.

collective motions of the whole cylinder. As noted in the TEM images, there are two types of disorder with different length scales on the Si nanowire surface—the first is a native amorphous oxide film which is characterized by the thickness, and the second is surface roughness, which can be characterized by a root-mean-square (rms) height. Let h be the length scale associated with this disordered region, which is the larger of the two above length scales (thickness and rms height). TEM images suggest the oxide layer is perhaps thicker than the rms height, and we denote this as $h = 2$ nm. To understand scattering from the boundary, we adopt a scalar wave model with $\omega = ck$, where c is the bulk sound velocity and k is the phonon wave vector. The quantity $k_\perp = \sqrt{k^2 - k_z^2}$ can be interpreted as the component of k that is perpendicular to the nanowire axis z, i.e., $k_\perp = k\cos\theta$ (see Fig. 3). One can argue that for $hk_\perp \leq 1$, the phonon should scatter specularly from the boundary [28]. When the wave is incident on the disordered boundary, the maximum path length difference in the specularly reflected component will be $2h\cos\theta$. If this path length difference is much shorter than the wavelength, then the specularly reflected component is not destroyed by interference effects.

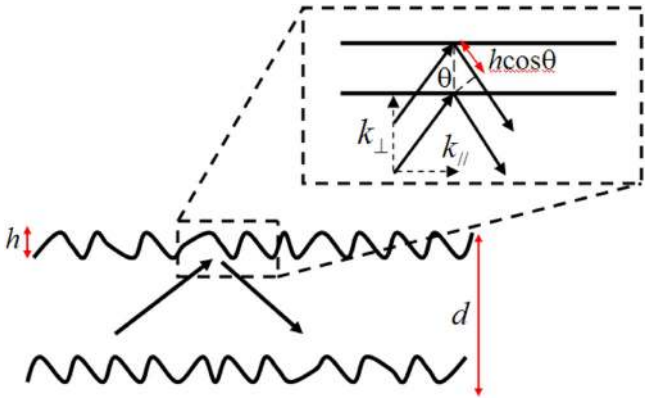

FIG. 3 (color online). Schematic diagram of the nanowire boundary used in the model. For phonon modes with $hk_\perp \ll 1$, if $k_\perp = k\cos\theta$ as shown, the path length difference is much shorter than the wavelength, so the specularly reflected component is not destroyed by interference effects. The mean free path of such specularly reflected phonon modes is given in Eq. (1).

However, modes for which $hk_\perp \leq 1$ are not fully ballistic. As discussed in Ref. [29], the mode with $k_\perp = 0$ is scattered with the frequency dependent inverse mean free path

$$l^{-1} = B\left(\frac{h}{d}\right)^2 \frac{1}{d}\left(\frac{\omega}{\omega_D}\right)^2 N(\omega), \tag{1}$$

where d is the diameter of the wire, ω is the frequency of the mode, ω_D is the Debye frequency, and $N(\omega)$ is the number of modes with frequency ω. B is a dimensionless constant that depends on the details of the disorder.

We therefore divide the modes at a given frequency into two groups: those with $hk_\perp \leq 1$, to which we assign the mean free path given by Eq. (1), and those with $hk_\perp > 1$ where diffusive transport is applicable, to which we assign a mean free path of d. We model the number of modes at a given frequency by

$$N(\omega) = 4 + A\left(\frac{d}{a}\right)^2\left(\frac{\omega}{\omega_D}\right)^2. \tag{2}$$

Here a is the lattice spacing, and the initial "4" gives the four modes (one longitudinal, one torsional and two flexural) that propagate as $\omega \to 0$; A is a dimensionless constant. The total number of modes can be split into the number of modes with mean free path l, $N_1(\omega)$, and the number with a mean free path of d, $N_2(\omega)$. $N_1(\omega)$ is given by $N(\min(\omega, c/h))$. At low frequencies all modes have $hk_\perp \leq 1$, whereas any modes that begin to propagate at $\omega > c/h$ are assumed to have $hk_\perp > 1$. $N_2(\omega)$ is defined by $N_2(\omega) = N(\omega) - N_1(\omega)$. The thermal conductance is then given by the Landauer formula [29]

$$G = \frac{1}{2\pi\hbar}\int_0^\infty \left(\frac{N_1(\omega)}{1 + L/\ell(\omega)} + \frac{N_2(\omega)}{1 + L/d}\right)\frac{\hbar^3\omega^2}{k_B T^2} \times \frac{e^{\hbar\omega/k_B T}}{(e^{\hbar\omega/k_B T} - 1)^2} d\omega, \quad (3)$$

where L is the length of the nanowire.

To fit the data we fix values for the dimensionless constants A and B; the same values are then used to model all the nanowires. For A, we choose 2.7, for B, 1.2, which are, as expected, of order unity [29]. The fit is shown in Fig. 2 (a) and its inset. The curves obtained from the model are in excellent agreement with the experimental results of all the six thin SiNW samples at low temperature. At high temperatures, the theoretical curves consistently overestimate the thermal conductance [Fig. 2(a)]. This is presumably due to the *umklapp* scattering that has not been included in the theoretical model. Also, one expects deviations from the ω^2 density of states at higher frequencies.

At low temperature, the unusual linear behavior of the $G(T)$ is a result of the competition between the two phonon transmission regimes: the specularly scattered modes (i.e., $hk_\perp \leq 1$) give a mean free path that scales like ω^{-4}; the other modes have mean free path of d. The distinction between the two phonon transmission regimes discussed here were absent in previous models on nanowires [13–16]. For thick nanowires, it is still appropriate to ignore the specularly scattered modes since the other modes contribute most to the thermal conductance [8–16]. However, for sufficiently thin nanowires, the contribution from the specularly scattered modes is significant and ignoring them would result in a significant mismatch with the experimental data, such as the model in Ref. [16] for the 22 nm SiNW in Ref. [8]. The present model, therefore, is especially appropriate for thin nanowires.

In summary, we have measured the thermal conductance $G(T)$ of silicon nanowires with diameters below 30 nm. The observed $G(T)$ scales linearly with temperature in the range of 20 to 100 K, as opposed to the T^3 dependence predicted by conventional phonon transport models., A theoretical model for this data suggests that the phonon-boundary scattering in thin SiNWs is frequency dependent, and ranges from nearly ballistic to completely diffusive for different modes. The competition between different phonon modes results in the observed linear behavior of $G(T)$ at low temperature. The new understanding obtained from the present study on phonon transport in NWs may have practical applications, such as in NW thermoelectrics and electronics thermal management.

This work was supported by the Division of Materials Sciences and Engineering, Office of Basic Energy Sciences, DOE. The authors would like to thank Professor Deyu Li and Dr. Chih-Wei Chang for helpful discussion. R. C. and A. I. H. wish to thank ITRI-Taiwan and the NSF-IGERT programs, respectively, for support. The authors also thank the National Center for Electron Microscopy and the UC Berkeley Microlab for use of their facilities.

*Corresponding author.
majumdar@me.berkeley.edu

[1] Y. Xia *et al.*, Adv. Mater. **15**, 353 (2003).
[2] D. J. Sirbuly *et al.*, J. Phys. Chem. B **109**, 15190 (2005).
[3] Y. Cui and C. M. Lieber, Science **291**, 851 (2001).
[4] Y. Nakayama *et al.*, Nature (London) **447**, 1098 (2007).
[5] X. Sun, Z. Zhang, and M. S. Dresselhaus, Appl. Phys. Lett. **74**, 4005 (1999); A. I. Hochbaum *et al.*, Nature (London) **451**, 163 (2008); A. I. Boukai *et al.*, Nature (London) **451**, 168 (2008).
[6] M. Law *et al.*, Nature Mater. **4**, 455 (2005).
[7] P. Kim *et al.*, Phys. Rev. Lett. **87**, 215502 (2001); M. Fujii *et al.*, Phys. Rev. Lett. **95**, 065502 (2005); C. Yu *et al.*, Nano Lett. **5**, 1842 (2005); C. W. Chang *et al.*, Phys. Rev. Lett. **97**, 085901 (2006).
[8] D. Li *et al.*, Appl. Phys. Lett. **83**, 2934 (2003).
[9] D. Li *et al.*, Appl. Phys. Lett. **83**, 3186 (2003).
[10] J. Zhou *et al.*, Appl. Phys. Lett. **87**, 133109 (2005).
[11] L. Shi *et al.*, Appl. Phys. Lett. **84**, 2638 (2004).
[12] O. Bourgeois *et al.*, J. Appl. Phys. **101**, 016104 (2007).
[13] S. G. Volz and G. Chen, Appl. Phys. Lett. **75**, 2056 (1999).
[14] J. Zou and A. Balandin, J. Appl. Phys. **89**, 2932 (2001).
[15] N. Mingo, Phys. Rev. B **68**, 113308 (2003).
[16] Y. Chen *et al.*, J. Heat Transfer **127**, 1129 (2005).
[17] I. Ponomareva, D. Srivastava, and M. Menon, Nano Lett. **7**, 1155 (2007).
[18] M. J. Biercuk *et al.*, Appl. Phys. Lett. **80**, 2767 (2002).
[19] The dominant phonon wavelength scales as $\lambda_{\max} \sim hc/k_B T$, where h is the Plank constant, c is the group velocity of phonon, k_B is the Boltzmann constant and T is the temperature. $\lambda_{\max}$ is larger for lower T.
[20] A. V. Zhukov *et al.*, JETP Lett. **81**, 190 (2005).
[21] A. L. Moore *et al.*, Appl. Phys. Lett. (to be published).
[22] Y. Wu and P. Yang, J. Am. Chem. Soc. **123**, 3165 (2001).
[23] A. I. Hochbaum *et al.*, Nano Lett. **5**, 457 (2005).
[24] E. Garnett, W. Liang, and P. Yang, Adv. Mater. **19**, 2946 (2007).
[25] L. Shi *et al.*, J. Heat Transfer **125**, 881 (2003).
[26] K. Schwab *et al.*, Nature (London) **404**, 974 (2000).
[27] M. G. Holland, Phys. Rev. **132**, 2461 (1963).
[28] J. A. Ogilvy and H. M. Merklinger, J. Acoust. Soc. Am. **90**, 3382 (1991).
[29] P. Murphy and J. Moore, Phys. Rev. B **76**, 155313 (2007).